



Contents lists available at ScienceDirect

Chemical Engineering and Processing: Process Intensification

journal homepage: www.elsevier.com/locate/cep

Recrystallization of pharmaceuticals using the batch supercritical anti-solvent process

Chie-Shaan Su, Muoi Tang, Yan-Ping Chen*

Department of Chemical Engineering, National Taiwan University, Taipei, Taiwan, ROC

ARTICLE INFO

Article history:

Received 22 April 2006

Received in revised form 12 February 2008

Accepted 13 February 2008

Available online xxx

Keywords:

Supercritical anti-solvent

Pharmaceutical

Volume expansion

ABSTRACT

Recrystallization of five pharmaceutical compounds using the batch supercritical anti-solvent (SAS) process was investigated in this study. The operation pressure was determined to be in the feasible region using the equation of state method. After the batch SAS process, significant modification of the crystal habits was observed from the SEM images. The recrystallized pharmaceuticals maintained similar crystalline structures after the batch process, as determined from the XRD analysis, but weaker intensities were observed in the XRD patterns. One endothermic peak for mefenamic acid was shifted after the batch SAS process due to particle size reduction or change in crystal habits.

© 2008 Published by Elsevier B.V.

1. Introduction

Supercritical fluid (SCF) technology is recognized as a green process that has been investigated in various fields of extraction, reaction, chromatography, and particle formation [1]. Carbon dioxide is the most commonly used supercritical fluid owing to its relatively low critical properties and the safety advantages. In recent years, particle formation technologies using SCF have extensively been discussed in pharmaceutical applications. Various particle formation techniques using SCF have been presented in literature [2]. Among those methods, supercritical anti-solvent (SAS) is the most widely used process [3,4]. In the SAS process, supercritical fluid is used as an anti-solvent to reduce the saturated solubility of solute and to cause particle formation in a short time period. In general, particle with specific crystal properties are obtained from the batch SAS process while smaller and amorphous particles are received from the continuous SAS process. For example, Yeo et al. [5] recrystallized two pharmaceuticals of sulfathiazole and chlorpropamide using the batch SAS process. Crystal habit, crystallinity and particle size were manipulated easily by changing the operation conditions. In our previous study [6], recrystallization and micronization of the non-steroidal anti-inflammatory drug (NSAID) salicylamide was demonstrated using the batch SAS process. After the SAS treatment, micronized pharmaceuticals may contribute to higher dissolution rate, less side effects and lower dosage requirement [3]. The SAS process has also been used for the production of microcapsules in controlled release applications [7].

In the SAS process, carbon dioxide is the most acceptable anti-solvent species. Particle size and crystal properties of pharmaceutical are easily manipulated by process parameters with no solvent residual in the final product. After charging the high pressure CO₂ into the solution, volumetric properties of the mixture change significantly due to rapid volume expansion. An accurate determination of the volumetric behavior for mixtures with high pressure CO₂ is important to the proper selection of solvent for the SAS process. Measurements and calculations for the volumetric properties in the equilibrium liquid phase have been presented in literature [8–10] using the Peng-Robinson equation of state (EOS). It is desirable to improve the volumetric calculations at high pressures by employing other EOS with superior ability in determining the volumes of pure solvents.

In this study, a batch SAS process was employed for the recrystallization of pharmaceuticals of phenacetin, mefenamic acid, gallic acid, carbamazepine and nitrofurantoin. The experimental temperature was 308.15 K. The operation pressure was determined where the volume expansion was high enough to favor the micronization of pharmaceutical particles. The Soave-Redlich-Kwong (SRK) [11], Peng-Robinson (PR) [12] and Volume-Translated Peng-Robinson (VTPR) [13] EOS with two-parameter van der Waals (VDW2) mixing rules were applied for calculating the composition, density and volume expansion in the anti-solvent expanded liquid phases. Comparisons of volumetric property calculation results are presented for commonly used organic solvents under elevated pressures. The most accurate EOS was further applied to calculate the relative molar volume change presented by de la Fuente Badilla et al. [9,14] in order to determine the operation pressures. After conducting the batch processes of five pharmaceutical compounds, the changes of crystal properties were compared and discussed.

* Corresponding author. Fax: +886 2 2362 3040.
E-mail address: ypchen@ntu.edu.tw (Y.-P. Chen).

2. Materials and methods

2.1. Thermodynamic models

In the SAS process, the anti-solvent CO₂ was charged into the liquid phase. It caused the volume expansion of solution and hence the particle precipitation in a short time period. The total volume of the liquid phase increased sharply near the critical pressure for the mixture of the solvent and CO₂ [8]. A proper selection of solvent/anti-solvent system with higher volume expansion at an acceptable pressure is essential to the SAS process. In this study, calculations of the total volume expansion ratio for a binary mixture of CO₂ with a commonly used solvent were firstly investigated. The total volume expansion ratio was defined as [8]:

$$\frac{\Delta V}{V} = \frac{V_L(T, P, x_1) - V_2(T, P_0)}{V_2(T, P_0)} \quad (1)$$

where $V_2(T, P_0)$ is the original total volume of pure solvent at a specific temperature and reference pressure (usually at 1 atm). $V_L(T, P, x_1)$ is the total volume of equilibrium liquid phase in a binary mixture. x_1 is the equilibrium mole fraction of carbon dioxide (component 1) dissolved in the liquid phase. Eq. (1) was also written as a function of density for practical calculations [9]:

$$\frac{\Delta V}{V} = \frac{\rho_2(T, P_0)}{\rho_L(T, P, x_1)} \left(\frac{x_1}{1 - x_1} \frac{M_1}{M_2} + 1 \right) - 1 \quad (2)$$

where M_1 and M_2 are the molecular weights of carbon dioxide and solvents, respectively. Flash calculations were employed in this study to calculate the vapor–liquid equilibrium (VLE) and volumetric properties for binary mixtures of CO₂ with commonly used solvents.

The SRK, PR and VTPR EOS were employed in this study for calculating the composition, density and total volume expansion ratio of the equilibrium liquid phase. The former two equations were widely used in engineering calculations. The VTPR EOS yielded improved volumetric results for pure fluids and was included in this high pressure calculation. Table 1 lists these EOS and their parameters. For mixture calculations, the van der Waals mixing rules with two parameters (VDW2) were employed. The mixture parameters

Table 1
Equations of state employed in this study

Equation of state	Parameters
Soave-Redlich-Kwong (SRK) equation of state $P = \frac{RT}{v-b} - \frac{a(T)}{v(v+b)}$	$a(T) = 0.42747 \frac{R^2 T_c^2}{P_c} \alpha(T)$
	$\alpha(T) = \left[1 + \kappa \left(1 - \sqrt{\frac{T}{T_c}} \right) \right]^2$
	$\kappa = 0.480 + 1.574\omega - 0.176\omega^2$
	$b = 0.08664 \frac{RT_c}{P_c}$
Peng-Robinson (PR) equation of state $P = \frac{RT}{v-b} - \frac{a(T)}{v(v+b) + b(v-b)}$	$a(T) = 0.45724 \frac{R^2 T_c^2}{P_c} \alpha(T)$
	$\alpha(T) = \left[1 + \kappa \left(1 - \sqrt{\frac{T}{T_c}} \right) \right]^2$
	$\kappa = 0.37464 + 1.54226\omega - 0.26992\omega^2$
	$b = 0.07780 \frac{RT_c}{P_c}$
Volume-Translated Peng-Robinson (VTPR) equation of state $P = \frac{RT}{v+t-b} - \frac{a(T)}{(v+t)(v+t+b) + b(v+t-b)}$	$a(T) = 0.45724 \frac{R^2 T_c^2}{P_c} \alpha(T)$
	$\alpha(T) = \left[1 + \kappa \left(1 - \sqrt{\frac{T}{T_c}} \right) \right]^2$
	$\kappa = 0.37464 + 1.54226\omega - 0.26992\omega^2$
	$b = 0.07780 \frac{RT_c}{P_c}$
	$t = 0.252 \frac{RT_c}{P_c} (Z_c - \chi)$
	$\chi = 2.5448Z_c - 0.4024$

Table 2
Data references of binary mixtures for CO₂ with various solvents

Solvent	T (K)	P (MPa)	Data points	Ref.
n-Pentane	277.65	0.23–3.75	10	[28]
n-Hexane	273.15–303.15	1.07–6.11	24	[29]
Cyclohexane	344.30	6.9–10.97	15	[27]
Benzene	344.30	6.9–10.96	16	[27]
Ethanol	298.15	1.55–5.90	18	[8]
Propionic acid	298.15–333.15	1.01–10.50	22	[26]
Ethyl Acetate	298.15–313.15	0.46–6.65	40	[8]
Acetone	298.15–313.15	1.01–8.00	15	[25,26]
Acetonitrile	298.15–313.15	0.49–7.81	42	[8]
Dimethyl sulfoxide	298.15–303.15	0.41–6.59	33	[8]

a_m and b_m in these EOS are:

$$a_m = \sum_i \sum_j x_i x_j a_{ij} \quad (3)$$

$$a_{ij} = \sqrt{a_i a_j} (1 - k_{ij}) \quad (4)$$

$$b_m = \sum_i \sum_j x_i x_j b_{ij} \quad (5)$$

$$b_{ij} = \frac{b_i + b_j}{2} (1 - l_{ij}) \quad (6)$$

In the VTPR EOS, the translated volume of a mixture (t_m) was a linear combination of pure fluid parameters:

$$t_m = \sum_i x_i t_i \quad (7)$$

The optimal binary interaction parameters k_{ij} and l_{ij} in the VDW2 mixing rules were determined by minimizing the calculated deviations of composition (x_1) and density (ρ_L) of the equilibrium liquid phase of the binary mixture. The objective function (O.F.) was the summation of absolute deviations over all data points:

$$\text{O.F.} = \frac{100}{N} \sum_{k=1}^N \left| \frac{x_{1,k}^{\text{cal}} - x_{1,k}^{\text{exp}}}{x_{1,k}^{\text{exp}}} \right| + \frac{100}{N} \sum_{k=1}^N \left| \frac{\rho_{L,k}^{\text{cal}} - \rho_{L,k}^{\text{exp}}}{\rho_{L,k}^{\text{exp}}} \right| \quad (8)$$

Table 2 lists the temperature and pressure ranges and the VLE data sources for the binary mixtures investigated in this study. Most of the commonly used solvents for the SAS process are included. The physical properties required in evaluating the pure fluid EOS parameters are presented in Table 3.

2.2. Selection of the appropriate operation conditions

Although the total volume expansion ratio is apparent for selecting the appropriate solvent and operation conditions, de la Fuente Badilla et al. demonstrated that the relative molar volume change

Table 3
Physical properties of pure solvents

Solvent	T_c (K) [30]	P_c (kPa) [30]	ω [30]	Z_c [13]
Carbon dioxide	304.12	7374	0.225	0.2741
n-Pentane	469.70	3370	0.252	0.2623
n-Hexane	507.60	3025	0.300	0.2644
Cyclohexane	553.50	4073	0.211	0.2729
Benzene	562.05	4895	0.210	0.2712
Ethanol	513.92	6148	0.649	0.2484
Propionic acid	604.00	4530	0.539	0.2070 [30]
Ethyl Acetate	523.20	3830	0.361	0.2518
Acetone	508.10	4700	0.307	0.2326
Acetonitrile	545.50 [31]	4850 [31]	0.327 [31]	0.1850 [31]
Dimethyl sulfoxide	720.00	5705	0.350	0.2148

ω is the acentric factor, and Z_c is the critical compressibility factor.

is more suitable for selecting the optimum thermodynamic conditions of the SAS process [9,14]. The relative molar volume change was defined as [9]:

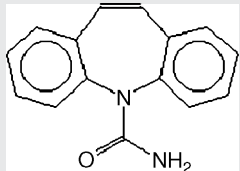
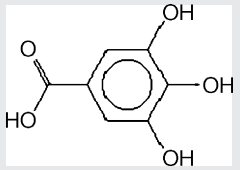
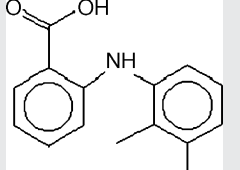
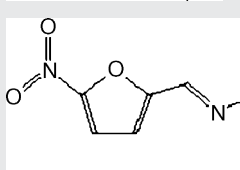
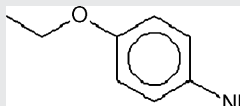
$$\frac{\Delta v}{v} = \frac{v_1(T, P, x_1) - v_2(T, P_0)}{v_2(T, P_0)} \quad (9)$$

where $v_2(T, P_0)$ is molar volume of a pure solvent at a specific temperature and reference pressure (usually at 1 atm). $v_1(T, P, x_1)$ is the molar volume of the equilibrium liquid phase in a binary mixture. x_1 is the equilibrium mole fraction of carbon dioxide dissolved in the liquid phase. The strategy purposed by de la Fuente et al. [14] was employed in this study for determining a proper operation pressure in our batch SAS experiments.

2.3. Materials

Phenacetin ($C_{10}H_{13}NO_2$), mefenamic acid ($C_{15}H_{15}NO_2$), carbamazepine ($C_{15}H_{12}N_2O$), gallic acid ($C_7H_6O_5$), and nitrofurantoin ($C_8H_6N_4O_5$) were purchased from the Sigma–Aldrich with purity greater than 99 mass%. Acetone (99.8 mass%), ethanol (99.8 mass%), ethyl acetate (99.8 mass%) and dimethyl sulfoxide (DMSO) (99.8 mass%) were used as the solvents in our experiments. Carbon dioxide (San Fu Co., Taiwan) was used as the anti-solvent with purity better than 99.5 mass%. The structures and physical properties of these pharmaceuticals are listed in Table 4. All chemicals were used without further purification.

Table 4
Structures and physical properties of pharmaceuticals investigated in this study

Compound	Structure	Properties [32]
Carbamazepine		Formula: $C_{15}H_{12}N_2O$; molecular weight: 236.27; melting point: 191–192 °C; drug utilization: anticonvulsant
Gallic acid		Formula: $C_7H_6O_5$; molecular weight: 170.12; melting point: 251 °C; drug utilization: antioxidant
Mefenamic acid		Formula: $C_{15}H_{15}NO_2$; molecular weight: 241.28; melting point: 230–231 °C; drug utilization: NSAID
Nitrofurantoin		Formula: $C_8H_6N_4O_5$; molecular weight: 238.16; melting point: 270–272 °C; drug utilization: antibacterial agent
Phenacetin		Formula: $C_{10}H_{13}NO_2$; molecular weight: 179.22; melting point: 134–135 °C; drug utilization: NSAID

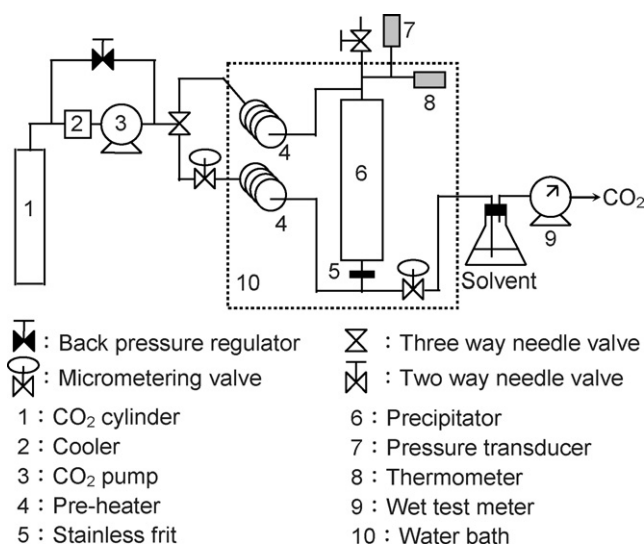


Fig. 1. Experimental apparatus of the batch SAS process.

2.4. Apparatus and procedures

The schematic diagram of the experimental apparatus for the batch SAS process is shown in Fig. 1. This system consists of three sections for carbon dioxide supply, recrystallization, and depressurization. High-pressure carbon dioxide was fed into the system directly from the gas cylinder or through a HPLC pump (SSI, series

II). A precipitator in the recrystallization section consisted of stainless steel tube, reducing union and stainless steel frits with different pore sizes (0.1 and 0.5 μm). Volume of the precipitator was 75 mL. In the depressurization section, a metering valve was used to control the gas flow rate, a cold trap was used for solvent recovery, and a wet test meter (Ritter, TG1) was used to record the flow rate of CO_2 .

In this study, 3 mL solution of pharmaceutical at 100% saturation was prepared and charged into the precipitator. Temperature in the precipitator was controlled at a desired value in a water bath with an accuracy of ± 0.1 K. Temperature and pressure in the precipitator were measured by thermocouple and pressure transducer with resolution of 0.01 K and 0.1 bar, respectively. The temperature and final pressure in the batch SAS process were controlled at 308.15 K and 10 MPa, respectively. Carbon dioxide was injected from the bottom of the precipitator after the system had reached thermal equilibrium. The pressurization time of 20 s from atmospheric to the final pressure of 10 MPa was regulated by a micrometering valve (Autoclave). The pharmaceutical compounds recrystallized in the volume expansion process. After the recrystallization step, supercritical drying was adopted to remove any residual solvent where carbon dioxide flowed through the top of the precipitator and left from the bottom continuously for 3–4 h. The precipitator was then depressurized to ambient pressure and the recrystallized pharmaceutical particles were collected from the stainless frits for further analyses.

2.5. Analytical methods

Crystal habits of pharmaceutical particles before and after the SAS process were examined using scanning electron microscope (SEM, JOEL JSM-6300). The crystal structures of pharmaceutical particles were analyzed by X-ray diffractometer (XRD, Philips X'pert diffractometer) between 5° and 80° with a scanning rate of 5°min^{-1} . Heat variation of phase transition of pharmaceutical compounds was measured by differential scanning calorimetry (DSC, DuPont TA 2010) with a heating rate of 10 K/min.

3. Results and discussion

3.1. Results for thermodynamic calculations

Thermodynamic modeling of the SAS process is useful in interpreting the experimental results at various operating conditions. Owing to the very low and limited solubility data for solid pharma-

Table 5

Binary interaction parameters from various equations of state and the VDW2 mixing rules

Solvents (component <i>j</i>)	SRK EOS		PR EOS		VTPR EOS	
	k_{ij}	l_{ij}	k_{ij}	l_{ij}	k_{ij}	l_{ij}
<i>n</i> -Pentane	0.078	−0.058	0.074	−0.056	0.076	−0.054
<i>n</i> -Hexane	0.105	−0.031	0.097	−0.030	0.097	−0.030
Cyclohexane	0.119	−0.006	0.111	−0.031	0.110	−0.026
Benzene	0.071	−0.003	0.066	−0.041	0.068	−0.034
Ethanol	0.098	0.012	0.100	0.008	0.106	0.014
Propionic acid	0.015	−0.018	0.022	−0.017	0.012	−0.030
Ethyl acetate	0.086	0.136	0.022	0.057	0.012	0.042
Acetone	0.113	0.158	0.056	0.059	0.026	0.020
Acetonitrile	0.076	0.057	0.080	0.058	0.089	0.072
Dimethyl sulfoxide	0.001	−0.035	0.008	−0.036	0.007	−0.038

Component 1 is carbon dioxide.

ceutical compounds in supercritical CO_2 , only few thermodynamic modeling for the phase behavior of the ternary mixture of supercritical CO_2 , solvent and pharmaceutical appeared in literature [15]. In this study, we focused on the calculated accuracy from EOS for density and total volume expansion in the equilibrium liquid phase of binary mixtures of supercritical CO_2 and solvent. These results are useful in selecting feasible operation conditions for the SAS process.

Table 5 shows the optimally fitted binary interaction parameters in the VDW2 mixing rules for the binary mixtures of SCCO_2 with commonly used solvents. These parameters for the three EOS are all in reasonable magnitude. Table 6 presents the calculated results in liquid phase compositions, liquid density and total volume expansion ratio from various EOS. It is observed that although the average deviations in liquid compositions are comparably satisfactory from either EOS, the calculated volumetric properties are quite different. The traditional engineering SRK and PR EOS showed appreciable deviation in either the liquid density or total volume expansion ratio. The corresponding deviations in the total volume expansion ratio from these two EOS were larger than 25%. The VTPR EOS inherently considered the improvement on liquid density, and yielded the best results among all EOS. Fig. 2 shows graphically the density calculation for the binary mixture of CO_2 and acetonitrile where the VTPR EOS is obviously superior to other EOS. Fig. 3 presents the comparison of calculated total volume expansion ratio from three EOS for the binary mixture of CO_2 and ethyl acetate. The VTPR EOS is again satisfactory with the average deviation of 10%. Fig. 4 shows the calculated total volume expansion ratios for CO_2 with various solvents from the VTPR EOS where the calculated results agree well with experimental data.

Table 6

Calculation results of equilibrium liquid composition, density and the total volume expansion ratio

Solvent (component <i>j</i>)	ARDX (%)			ARDD (%)			ARDV (%)		
	SRK	PR	VTPR	SRK	PR	VTPR	SRK	PR	VTPR
<i>n</i> -Pentane	1.39	1.28	1.30	13.35	3.17	4.45	21.48	19.57	21.66
<i>n</i> -Hexane	1.06	0.87	0.88	13.43	2.68	4.61	8.69	9.02	10.21
Cyclohexane	2.54	0.44	0.69	5.99	0.89	2.19	11.68	7.78	4.52
Benzene	2.21	0.44	0.27	5.69	0.93	2.41	12.31	6.21	4.07
Ethanol	3.60	4.14	4.34	10.47	2.95	3.75	28.11	52.26	26.67
Propionic acid	8.24	2.36	2.96	8.07	10.81	4.90	40.13	34.90	12.49
Ethyl Acetate	5.90	4.40	4.57	7.26	1.36	0.36	38.65	19.86	10.97
Acetone	8.24	3.02	1.65	8.07	3.57	1.25	40.13	22.40	4.35
Acetonitrile	4.52	4.40	5.28	29.15	20.17	1.71	45.27	45.13	19.98
Dimethyl sulfoxide	11.09	11.36	11.34	24.53	15.38	0.65	24.47	27.33	23.09
	5.42	4.06	4.24	14.67	7.99	2.25	29.96	26.66	14.70

ARDX: absolute average relative deviation on liquid phase composition: $\text{ARDX} = (100/N) \sum_{k=1}^N \left| \frac{(x_{1,k}^{\text{cal}} - x_{1,k}^{\text{exp}})/x_{1,k}^{\text{exp}}}{x_{1,k}^{\text{exp}}} \right|$, x_1 is the mole fraction of CO_2 . ARDD: absolute average relative deviation on density of the anti-solvent expanded liquid phase: $\text{ARDD} = (100/N) \sum_{k=1}^N \left| \frac{(\rho_{L,k}^{\text{cal}} - \rho_{L,k}^{\text{exp}})/\rho_{L,k}^{\text{exp}}}{\rho_{L,k}^{\text{exp}}} \right|$, ρ_L is the density of anti-solvent expanded liquid phase.

ARDV: absolute average relative deviation on the total volume expansion of liquid phase: $\text{ARDV} = (100/N) \sum_{k=1}^N \left| \frac{(\Delta V/V)_k^{\text{cal}} - (\Delta V/V)_k^{\text{exp}}/(\Delta V/V)_k^{\text{exp}}}{(\Delta V/V)_k^{\text{exp}}} \right|$, $\Delta V/V$ is the total volume expansion ratio of the anti-solvent expanded liquid phase.

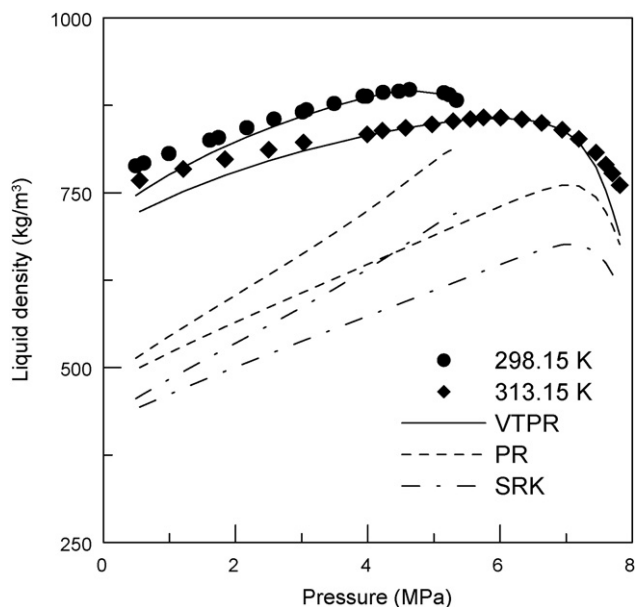


Fig. 2. Comparison of the calculated results of equilibrium liquid phase density for the binary mixture of CO₂ and acetonitrile using various equations of state.

It is shown in Fig. 4 that the total volume expansion occurred above a certain pressure for each binary mixture of CO₂ and solvent. An improved strategy for selecting the operation pressure was presented by de la Fuente et al. [14]. According to their results, the operation temperature should be closed to the critical point of the anti-solvent. The operation pressure was determined by plotting the relative molar volume change against pressure at the operating temperature. A minimum point at P_{min} was observed in the plot and a sharp increase of volume expansion existed above P_{min} . The relative molar volume change of solvents including acetone, dimethyl sulfoxide, ethanol and ethyl acetate were calculated using the VTPR EOS with optimally fitted parameters. The operation temperature of our SAS experiments was 308.15 K and was slightly higher than

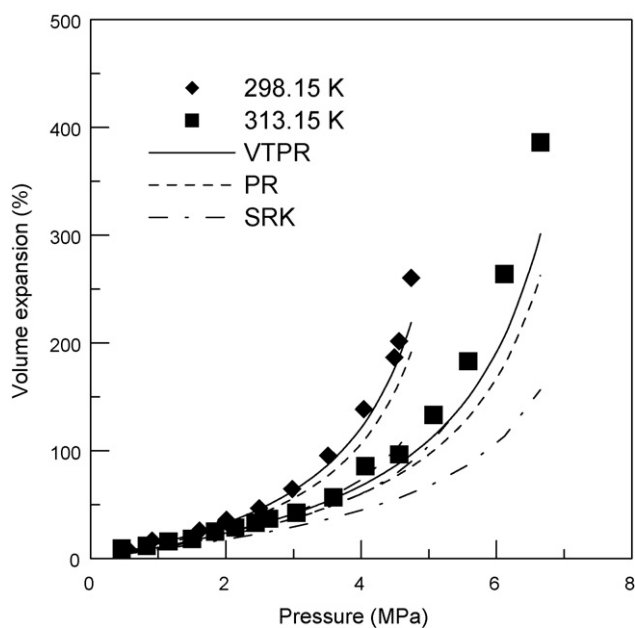


Fig. 3. Comparison of the calculated results of the total volume expansion for the binary mixture of CO₂ and ethyl acetate using various equations of state.

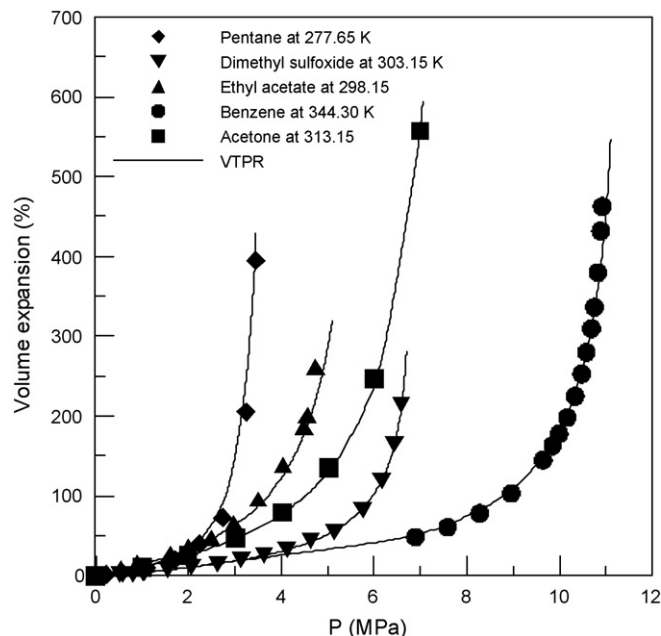


Fig. 4. Calculation results of the total volume expansion for binary mixtures of CO₂ and various solvents at specific temperatures.

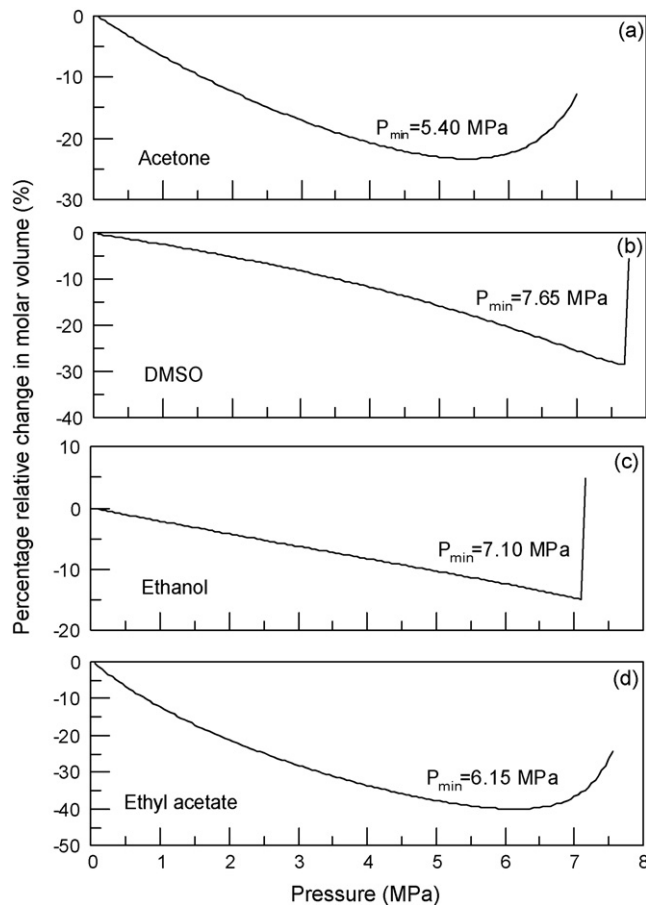


Fig. 5. Calculation results of relative molar volume change at 308.15 K using the VTPR EOS with optimally fitted parameters for solvents employed in this study (a) acetone, (b) dimethyl sulfoxide, (c) ethanol and (d) ethyl acetate.

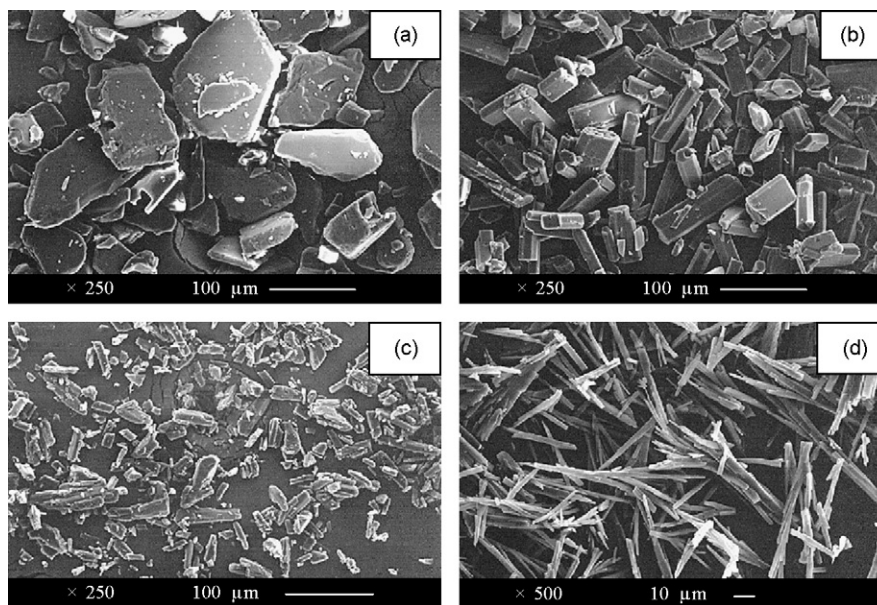


Fig. 6. SEM images of two non-steroidal anti-inflammatory drugs (a) original phenacetin, (b) phenacetin after the batch SAS process, (c) original mefenamic acid and (d) mefenamic acid after the batch SAS process.

the critical temperature of carbon dioxide. Fig. 5 shows the plots of the calculated relative molar volume change against pressure for four solutes at 308.15 K. A minimum point is observed for each solvent in Fig. 5. The P_{min} values are all less than 9 MPa. The operation

pressure of 10 MPa in our SAS experiments is above all P_{min} values. At this operation pressure, a high supersaturation condition of solute is expected for successful recrystallization and micronization of pharmaceutical particles.

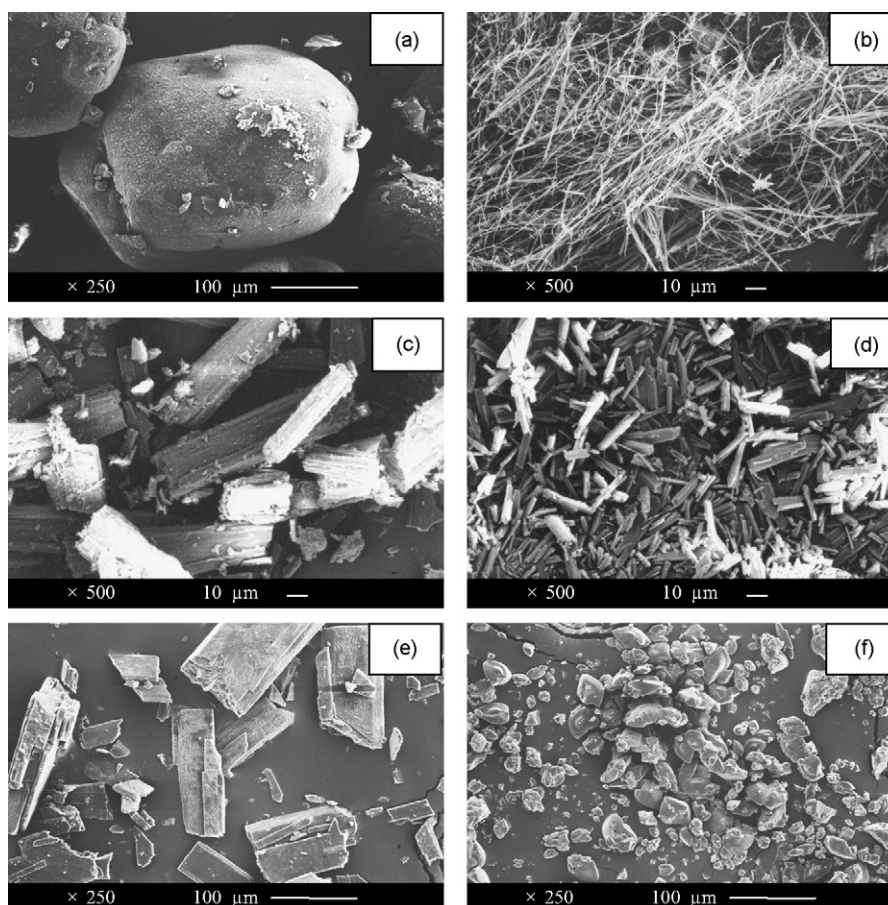


Fig. 7. SEM images of pharmaceuticals (a) original carbamazepine, (b) carbamazepine after the batch SAS process, (c) original gallic acid, (d) gallic acid after the batch SAS process, (e) original nitrofurantoin and (f) nitrofurantoin after the batch SAS process.

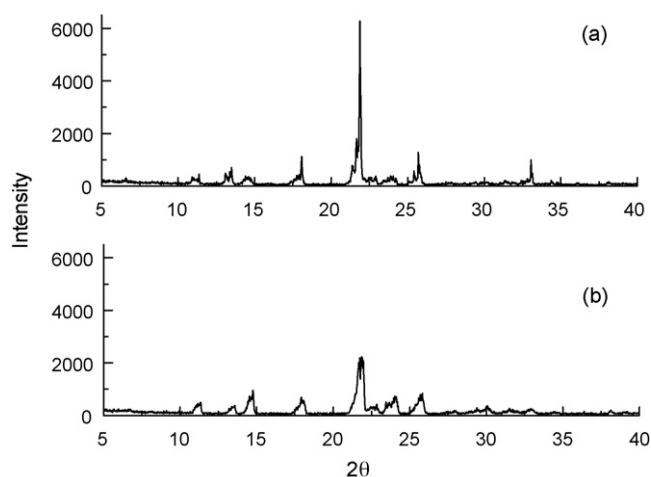


Fig. 8. XRD patterns of phenacetin (a) original and (b) after the batch SAS process.

3.2. Results for the batch SAS process

Modification of the crystal habits using the batch SAS process was demonstrated in this study. Fig. 6 shows the SEM images for the recrystallization of two non-steroidal anti-inflammatory drugs of phenacetin and mefenamic acid. The original shapes of these two compounds were irregular and broken, as shown in Fig. 6(a) and (c), respectively. After the batch SAS process using acetone as the solvent, particles of phenacetin show rectangular shape as depicted in Fig. 6(b). Fig. 6(d) shows that the needle-like mefenamic acid was observed after the batch SAS process using ethyl acetate as the solvent. Furthermore, three functional pharmaceuticals of carbamazepine (an anticonvulsant), gallic acid (an antioxidant), and nitrofurantoin (an antibacterial agent) were recrystallized using the batch SAS process and the results are presented in Fig. 7. The SEM images of the original compounds are also broken and irregular, as shown in Fig. 7(a), (c) and (e) for carbamazepine, gallic acid and nitrofurantoin, respectively. Fig. 7(b) shows the SEM image of carbamazepine after the batch SAS process using acetone as the solvent. The shape becomes fibrous that is very different from its original sample shown in Fig. 7(a). Fig. 7(d) shows that short rod-like gallic acid was received after the batch SAS process using ethanol as the solvent. Nitrofurantoin shows the similar effect in Fig. 7(f) after the batch SAS process using DMSO as the solvent where irregular, smaller and broken particles were obtained.

The crystalline structures of these pharmaceutical compounds were observed from the XRD patterns. Fig. 8(a) and (b) shows the example for the XRD patterns of phenacetin before and after the batch SAS process, respectively. The main peaks of the XRD spectrum still exist but the intensity of specific diffraction signal, for example at 2θ equals to 22° , was decreased significantly after the batch SAS process. A similar result was observed for the recrystallization of another pharmaceutical compound of salbutamol using the SAS process in literature [16]. In this study, similar results for the decrease of intensities in specific diffraction signals were obtained for the other four pharmaceuticals. The differences observed from XRD pattern could be due to a change in crystal size or habit. Fig. 9(a) and (b) shows the DSC measurement results for phenacetin before and after the SAS process, respectively. The DSC results shown in Fig. 9 are similar before and after the batch SAS process. The melting temperatures in both Fig. 9(a) and (b) are the same and are also consistent with that listed in literature [17]. All these results show that there is no deterioration of phenacetin during the batch SAS process.

The other compounds in this study, except for mefenamic acid, have the similar DSC results before and after the batch SAS pro-

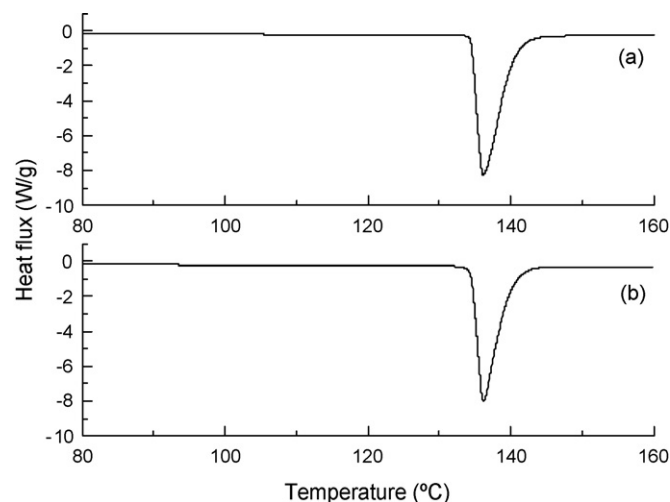


Fig. 9. DSC analysis results of pharmaceutical (a) original phenacetin and (b) phenacetin after the batch SAS process.

cesses. Fig. 10(a) and (b) presents the DSC measurement results of mefenamic acid where the melting temperature remained the same after the batch SAS treatment. Its value was consistent with that shown in literature [18]. Fig. 10(c) shows that the original mefenamic acid also has an endothermic peak with onset temperature

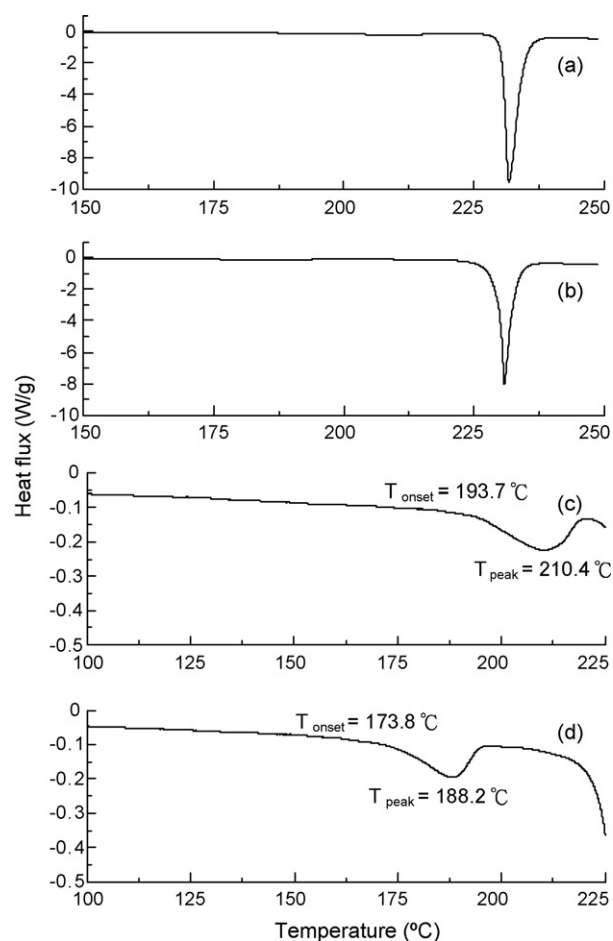


Fig. 10. DSC analysis results of pharmaceutical (a) melting temperature of original mefenamic acid, (b) melting temperature of mefenamic acid after the batch SAS process, (c) first endothermic peak of original mefenamic acid and (d) first endothermic peak of mefenamic acid after the batch SAS process.

at 197.3 °C before the melting point. The onset temperature of this endothermic peak changed to 173.8 °C after the batch SAS process, as depicted in Fig. 10 (d). It was presented by Umeda et al. [19] that a transition temperature at 179 °C existed for mefenamic acid. This transition temperature was also reported by Adam et al. [20] and Panchagnula et al. [21] using different commercial samples of mefenamic acid. For example, Panchagnula et al. [21] observed that the onset temperature of the first endotherm varied from 167 to 217 °C for various commercial samples. The change of the transition temperature observed in our SAS experiments may be attributed to the differences in solid state characteristics such as particle size, crystal habits and imperfections created in the crystals during the recrystallization process.

From the SEM images, XRD and DSC patterns for the five pharmaceutical compounds investigated in this study, it is demonstrated that their crystal properties were modified using the batch SAS process. These results are consistent with previous reports that the crystal habits of pharmaceuticals are manipulated in the SAS process [22,23]. In a recent literature, it was discussed that not only the micronized particle size is important to the dissolution of pharmaceutical compounds, the crystal or surface properties also have significant effects [24]. The experimental observations from this study supply information for future applications in pharmaceutical industry.

4. Conclusion

This study employed the EOS method to calculate the thermodynamic properties for fluid mixtures of CO₂ and various solvents. It is demonstrated that the VTPR EOS gave the superior calculation results for liquid density and the total volume expansion ratio to those from other commonly employed cubic EOS. The suitable operation pressure in the SAS process was further selected using the calculation result of the relative molar volume change from the VTPR EOS. Recrystallizations of pharmaceuticals using the batch SAS process are reported for phenacetin, mefenamic acid, carbamazepine, gallic acid and nitrofurantoin. The operation conditions are 308.15 K and 10 MPa that are appropriate from thermodynamic calculation results. Significant changes of crystal habits for each pharmaceutical compound were observed from the SEM images. Comparisons of the XRD patterns before and after the batch SAS process also indicated the modifications on specific crystal planes. The DSC measurements ensured that no deterioration occurred during the batch SAS process.

Acknowledgements

The authors are grateful to the support from the Ministry of Economic Affairs, and National Science Council, Taiwan, ROC.

Appendix A. Nomenclature

a, b	equation of state parameters
k, l	binary interaction parameters
M	molecular weight
N	number of components
P	pressure
t	parameter in the VTPR equation of state
T	temperature
v	molar volume
Δv	molar volume change
V	total volume
ΔV	total volume change
x	mole fraction

Z compressibility factor

Greek letters

α	temperature dependent parameter in the equations of state
χ	parameter in the equations of state
κ	parameter in the equations of state
ρ	density

Subscripts

c	critical properties
i, j, k	components i, j , and k
L	liquid phase property
m	mixture property
0	reference pressure, 1 atm
1	component 1, carbon dioxide
2	solvent

Superscripts

cal	calculated results
exp	experimental data

References

- [1] E.J. Beckman, Supercritical and near-critical CO₂ in green chemical synthesis and processing, *J. Supercrit. Fluids* 28 (2004) 121–191.
- [2] I. Pasquali, R. Bettini, F. Giordano, Solis state chemistry and particle engineering with supercritical fluids in pharmaceuticals, *Eur. J. Pharm. Sci.* 27 (2006) 239–310.
- [3] B. Subramaniam, R.A. Rajewski, K. Snavely, Pharmaceutical processing with supercritical carbon dioxide, *J. Pharm. Sci.* 86 (1997) 885–890.
- [4] P. York, Strategies for particle design using supercritical fluids technology, *Pharm. Sci. Technol. Today* 2 (1999) 430–440.
- [5] S.D. Yeo, M.S. Kim, J.C. Lee, Recrystallization of sulfathiazole and chlorpropamide using the supercritical fluid anti-solvent process, *J. Supercrit. Fluids* 25 (2003) 143–154.
- [6] C.S. Su, Y.P. Chen, Recrystallization of salicylamide using a batch supercritical antisolvent process, *Chem. Eng. Technol.* 28 (2005) 1177–1181.
- [7] L.S. Tu, F. Dehghani, N.R. Foster, Micronisation and microencapsulation of pharmaceuticals using a carbon dioxide antisolvent, *Powder Technol.* 126 (2002) 134–149.
- [8] A. Kordikowski, A.P. Schenk, R.M. Van Nielen, C.J. Peters, Volume expansion and vapor-liquid equilibrium of binary mixtures of a variety of polar solvents and certain near critical solvents, *J. Supercrit. Fluids* 8 (1995) 205–216.
- [9] J.C. de la Fuente Badilla, C.J. Peters, J. de Swaan Arons, Volume expansion in relation to the gas-antisolvent process, *J. Supercrit. Fluids* 17 (2000) 13–23.
- [10] M. Mukhopadhyay, Partial molar volume reduction of solvent for solute crystallization using carbon dioxide as antisolvent, *J. Supercrit. Fluids* 25 (2003) 213–223.
- [11] G. Soave, Equilibrium constants from a modified Redlich-Kwong equation of state, *Chem. Eng. Sci.* 27 (1972) 1197–1203.
- [12] D.Y. Peng, D.B. Robinson, A new two-constants equation of state, *Ind. Eng. Chem. Fundam.* 15 (1976) 59–64.
- [13] J. Ahlers, J. Gmehling, Development of an universal group contribution equation of state I. Prediction of liquid densities for pure compound with a volume translated Peng-Robinson equation of state, *Fluid Phase Equilib.* 191 (2001) 177–188.
- [14] J.C. de la Fuente, A. Shariati, C.J. Peters, On the selection of optimum thermodynamic conditions for the GAS process, *J. Supercrit. Fluids* 32 (2004) 55–61.
- [15] F. Miguel, A. Mart'n, T. Gamse, M.J. Cocero, Supercritical anti-solvent precipitation of lycopene: effect of the operating parameters, *J. Supercrit. Fluids* 36 (2006) 225–235.
- [16] E. Reverchon, G. Della Porta, P. Pallado, Supercritical antisolvent precipitation of salbutamol microparticles, *Powder Technol.* 114 (2001) 17–22.
- [17] S. Vecchio, A. Catalani, V. Rossi, M. Tomassetti, Thermal analysis study on vaporization of some analgesics. Acetanilide and derivatives, *Thermochim. Acta* 420 (2004) 99–104.
- [18] Y.A. Ribeiro, J.D.S. de Oliveira, M.I.G. Leles, S.A. Juiz, M. Ionashiro, Thermal decomposition of some analgesic agents, *J. Therm. Anal.* 46 (1996) 1645–1655.
- [19] T. Umeda, N. Ohnishi, T. Yokoyama, T. Kuroda, Y. Kita, K. Kuroda, E. Tatsumi, Y. Matsuda, A kinetic study on the isothermal transition of polymorphic forms of tolbutamide and mefenamic acid in the solid state at high temperature, *Chem. Pharm. Bull.* 35 (1985) 2073–2078.
- [20] A. Adam, L. Schrimpl, P.C. Schmidt, Some physicochemical properties of mefenamic acid, *Drug. Dev. Ind. Pharm.* 26 (2000) 477–487.
- [21] R. Panchagnula, P. Sundaramurthy, O. Pillai, S. Agrawal, Y.A. Raj, Solid-state characterization of mefenamic acid, *J. Pharm. Sci.* 93 (2004) 1019–1029.

- [22] S.D. Yeo, J.C. Lee, Crystallization of sulfamethizole using the supercritical and liquid antisolvent processes, *J. Supercrit. Fluids* 30 (2004) 315–323.
- [23] B. De Gioannis, P. Jestin, P. Subra, Morphology and growth control of griseofulvin recrystallized by compressed carbon dioxide as antisolvent, *J. Crystal Growth* 262 (2004) 519–526.
- [24] M. Perrut, J. Jung, F. Leboeuf, Enhancement of dissolution rate of poorly-soluble active ingredients by supercritical fluid processes. Part I: Micronization of neat particles, *Int. J. Pharm.* 288 (2005) 3–10.
- [25] M. Kato, K. Aizawa, T. Kanahira, T. Ozawa, A new experimental method of vapor-liquid equilibria at high pressures, *J. Chem. Eng. Jpn.* 24 (1991) 767–771.
- [26] T. Adrian, G. Maurer, Solubility of carbon dioxide in acetone and propionic acid at temperatures between 298 K and 333 K, *J. Chem. Eng. Data* 42 (1997) 668–672.
- [27] N. Nagarajan, R.L. Robinson Jr., Equilibrium phase compositions, phase densities, and interfacial tensions for CO₂+hydrocarbon systems. 3. CO₂+cyclohexane. 4. CO₂+benzene, *J. Chem. Eng. Data* 32 (1987) 369–371.
- [28] G.J. Besserer, D.B. Robinson, Equilibrium phase properties of *n*-pentane-carbon dioxide system, *J. Chem. Eng. Data* 18 (1973) 416–419.
- [29] G.I. Kaminishi, C. Yokoyama, S. Takahashi, Vapor pressure of binary mixtures of carbon dioxide with benzene, *n*-hexane and cyclohexane up to 7 MPa, *Fluid Phase Equilib.* 34 (1987) 83–99.
- [30] B.E. Poling, J.M. Prausnitz, J.P. O'Connell, *The Properties of Gases and Liquids*, fifth ed., McGraw-Hill, New York, 2001.
- [31] Korea Thermophysical Properties Data Bank (<http://infosys.korea.ac.kr/kdb/index.html>).
- [32] S. Budavari, M.J. O'Neil, A. Smith, P.E. Heckelman, J.F. Kinneary, *The Merck Index: An Encyclopedia of Chemicals, Drugs, and Biologicals*, 13th ed., Merck & Co., Inc., 2001.